JACS
JOURNAL OF THE AMERICAN CHEMICAL SOCIETY
pubs.acs.org/JACS
Article

Versatile Porous Poly(arylene ether)s via Pd-Catalyzed C–O Polycondensation

Sheng Guo and Timothy M. Swager*

Cite This: J. Am. Chem. Soc. 2021, 143, 11828–11835
Read Online
ACCESS | Metrics & More | Article Recommendations | Supporting Information

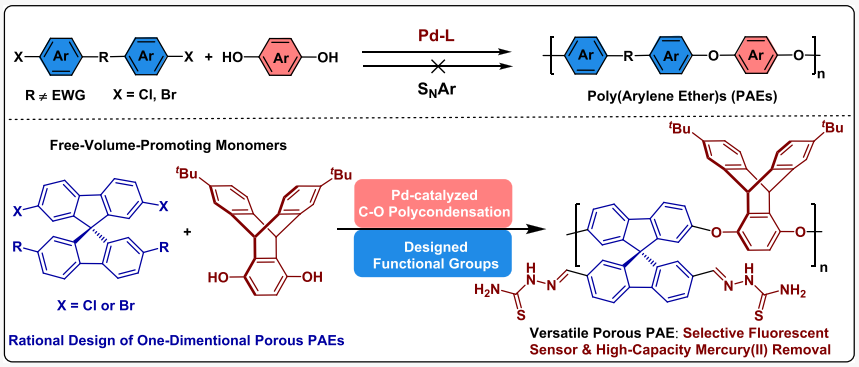

ABSTRACT: Porous organic polymers (POPs) with strong covalent linkages between various rigid aromatic structural units having different geometries and topologies are reported. With inherent porosity, predictable structure, and tunable functionality, POPs have found utility in gas separation, heterogeneous catalysis, sensing, and water treatment. Poly(arylene ether)s (PAEs) are a family of high-performance thermoplastic materials with high glass-transition temperatures, exceptional thermal stability, robust mechanical properties, and excellent chemical resistance. These properties are desirable for development of durable POPs. However, the synthetic methodology for the preparation of these polymers has been mainly limited in scope to monomers capable of undergoing nucleophilic aromatic substitution (S_NAr) reactions. Herein, we describe a new general method using Pd-catalyzed C–O polycondensation reactions for the synthesis of PAEs. A wide range of new compositions and PAE architectures are now readily available using monomers with unactivated aryl chlorides and bromides. Specifically, monomers with conformational rigidity and intrinsic internal free volume are now used to create porous organic polymers with high molecular weight, good thermal stability, and porosity. The reported porous PAEs are solution processable and can be used in environmentally relevant applications including heavy-metal-ion sensing and capture.

INTRODUCTION

Intrinsically porous organic polymers (POPs) are promising materials for gas separation, heterogeneous catalysis, sensing, water treatment, and other intriguing applications.[1−4] POPs can be amorphous (e.g., porous aromatic frameworks, polymers of intrinsic microporosity) or highly crystalline (e.g., covalent organic framework).[4] One-dimensional linear POPs are attractive as a result of their tunable porosity and solution processability[5−7] (Figure 1a). For example, the linear polymer PIM-1, reported by Budd and McKeown in 2004,[8] has been the subject of considerable research.[7] The many applications of POPs continue to motivate the design of novel linear polymers that are robust, solution processable, and highly porous.

Poly(arylene ether)s (PAEs) are an attractive platform for developing new POPs with long-term structural, thermal, and chemical stability.[9,10] We have previously shown that triptycenes and higher iptycenes create materials with free volume in a number of different contexts.[11−15] The scope of PAEs containing iptycenes and other free volume-promoting structural units was limited to materials that could be produced by S_NAr reactions, which requires one of the monomers to be an activated aryl fluoride (Figure 1b).[12,13] Specifically, efficient S_NAr reactions require the stabilization of a delocalized anionic intermediate or transition state, and it is common for monomers to have electron-withdrawing groups ortho or para to the aryl fluorides that are to be displaced. It is also the case that fluorides are often more reactive in S_NAr reactions than the more accessible chlorides or bromides, thereby limiting the scope of potential functional macromolecular

Received: June 6, 2021
Published: July 27, 2021

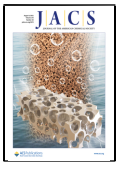

https://doi.org/10.1021/jacs.1c05853
J. Am. Chem. Soc. 2021, 143, 11828–11835

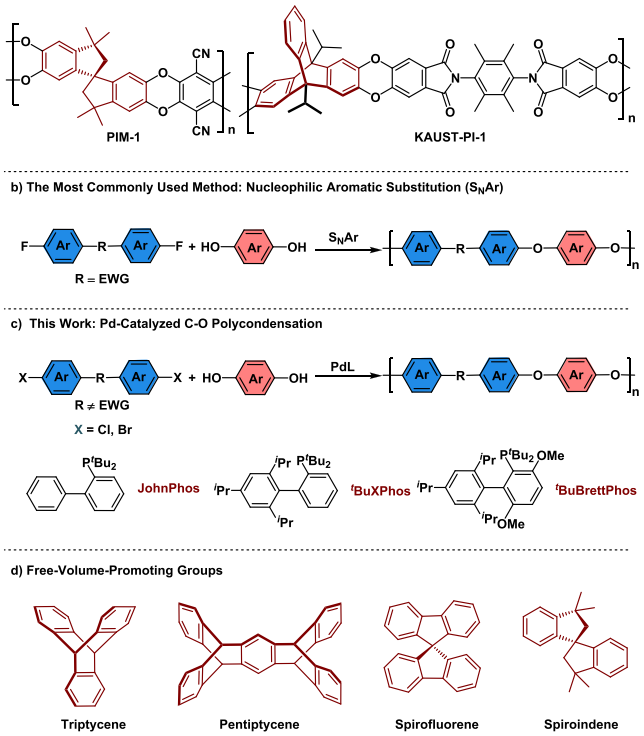

Figure 1. (a) Representative 1D porous organic polymers.[5,8] (b) Nucleophilic aromatic substitution. (c) Pd-catalyzed C−O polycondensation. (d) Free-volume-promoting groups.

architectures. We demonstrate herein that Pd-catalyzed C−O cross-coupling reactions remove these limitations and allow for the facile synthesis and a greatly expanded scope of PAEs. These methods are enabled by the use of sterically hindered, electron-rich biarylphosphine ligands, such as ^{t}BuXPhos, that promote Pd-catalyzed C−O cross-coupling reactions under mild conditions. Although Pd-catalyzed C−O cross-coupling reactions have been extensively studied in the context of diaryl ether synthesis,[16−18] they have not been used to produce high molecular weight PAEs.[19] Our new PAE synthesis allows for the use of aryl chlorides and bromides, which are readily available with a variety of substituent patterns (Figure 1c).

At the outset of this study, we hypothesized that a reaction enabling the use of two conformationally rigid and free-volume-promoting monomers in a polyether condensation reaction would produce POPs. We have selected monomers containing triptycene (Trip),[20] pentiptycene (Pentrip),[21] spirobifluorene (SBF),[22,23] and spiroindene (SBI)[24] to create polymers with enhanced rigidity and porosity (Figure 1d). These base structures do not include electron-deficient (activated) aryl fluorides required for S_NAr reactions, and PAEs are accessed by Pd-catalyzed C−O polycondensation reactions between bisphenols and aryl chlorides and bromides. This new route provides access to new solution-processable porous PAEs with a diversity of functional groups to create highly versatile materials.

RESULTS AND DISCUSSION

We began our studies by examining the reaction of activated aryl chlorides that were considered to be high-activity substrates for Pd-catalyzed C−O cross-coupling.[17] To determine the optimal reaction conditions for Pd-catalyzed C−O polycondensation reaction, the reaction of the more soluble Schiff base (ketimine) of 4,4′-dichlorobenzophenone and hydroquinone was investigated. This polycondensation reaction produces a soluble precursor of the well-known thermoplastic poly(ether ether ketone) (PEEK), which is generated by hydrolysis.[25,26] S_NAr reactions with aryl chloride monomers have been previously reported to be ineffective at producing PEEK and suffer from reductive dehalogenation chain-terminating side reactions.[27] These competing processes are suppressed with Pd catalysis, and dialkyl biarylphosphine ligands facilitate the polymerization. The use of JohnPhos and ^{t}BuBrettPhos in the polycondensation reaction afforded poly(ether ether ketimine) **P1** with low molecular weight (Table 1, entries 1 and 3). Continued optimization (120 °C, 2-MeTHF solvent, Table 1, entry 2) revealed that ^{t}BuXPhos is the optimal ligand for the polycondensation providing the PEEK precursor as a high molecular weight soluble polymer. A control experiment without Pd revealed that the S_NAr reactions are negligible under these conditions. In addition, we investigated the reaction of aryl bromides, which are more active than chlorides in oxidative addition reactions (Table 1, entry 7). We found that the use of ^{t}BuBrettPhos furnished **P1** with a high molecular weight (Table 1, entry 6). The results shown in Table 1 indicate that ^{t}BuXPhos is superior to ^{t}BuBrettPhos in the polycondensation of aryl chlorides. Alternatively, ^{t}BuBrettPhos is superior to ^{t}BuXPhos in the polycondensation of aryl bromides. The less sterically hindered ^{t}BuXPhos may be necessary to facilitate the ligand exchange of LPd(Ar)Cl with phenoxides in the coupling of aryl chlorides since Cl is more tightly bound to Pd than Br. In contrast, for aryl bromides, the more sterically hindered ^{t}BuBrettPhos can accelerate the reductive elimination step of the coupling more effectively than ^{t}BuXPhos.[16]

Table 1. Ligand Screening for Pd-Catalyzed Synthesis of Poly(arylene ether)s

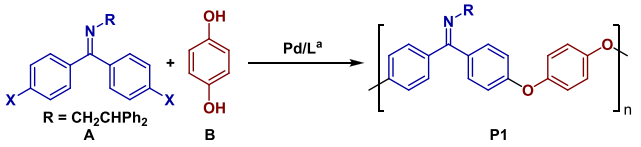

entry	X	ligand	M_n (kg/mol)[b]	$Đ$[b]	yield (%)[c]
1	Cl	JohnPhos	1.7	1.2	
2	Cl	^{t}BuXPhos	64.2	1.6	98
3	Cl	^{t}BuBrettPhos	10.3	1.6	95
4	Br	JohnPhos	2.1	1.3	
5	Br	^{t}BuXPhos	2.5	1.4	
6	Br	^{t}BuBrettPhos	57.8	1.9	98
7	Cl or Br	no Pd and L	0.4	1.0	

[a]Aryl halide **A** (0.5 mmol), bisphenol **B** (0.5 mmol), [(cinnamyl)-PdCl]$_2$ (0.5 mol %), ligand (3.0 mol %), K_3PO_4 (3.0 equiv), 2-MeTHF (1.0 mL), 120 °C, 72 h. [b]M_n and $Đ$ were measured by THF GPC. M_n = number-average molar mass. $Đ$ = molecular weight distribution. [c]Yield refers to isolated yield of purified polymer product.

Having identified the optimal reaction conditions for PEEK-related materials, we next investigated the synthesis of PAE-based POPs using bisphenols and aryl dihalides capable of promoting free volume. In this context, triptycene is an exceptionally reliable rigid nonplanar free-volume-promoting group, which has been shown to endow polymers with good solubility and high glass-transition temperatures.[11] Triptycene-

https://doi.org/10.1021/jacs.1c05853
J. Am. Chem. Soc. 2021, 143, 11828−11835

Table 2. Synthesis of Porous Poly(arylene ether)s via Pd-Catalyzed C−O Polycondensation

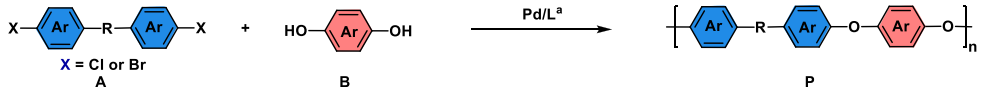

a) Synthesis of PAEs by using activated aryl chlorides or bromides

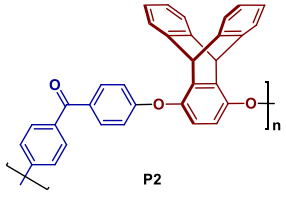

P2
X=Cl 95% yield
Mn = 30.5 kg/mol, *Đ* = 1.6

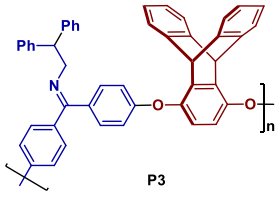

P3
X=Cl 96% yield
Mn = 59.3 kg/mol, *Đ* = 1.6

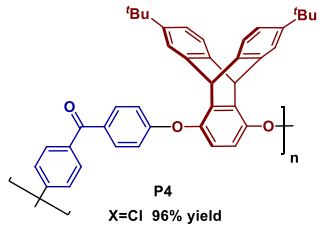

P4
X=Cl 96% yield
Mn = 46.3 kg/mol, *Đ* = 1.7
38 m^2/g^d

b) Synthesis of PAEs by using unactivated aryl chlorides or bromides

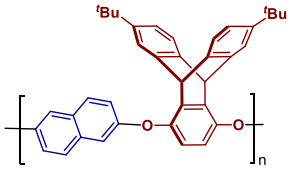

P5
X=Br 91% yield
Mn = 18.6 kg/mol, *Đ* = 1.6[b]
38 m^2/g^d

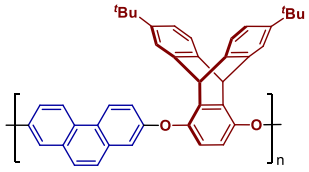

P6
X=Br 95% yield
Mn = 22.9 kg/mol, *Đ* = 1.9[b]
202 m^2/g^d

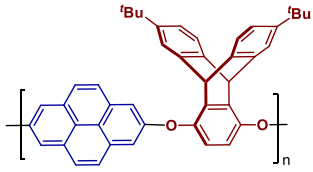

P7
X=Br 92% yield
Mn = 9.4 kg/mol, *Đ* = 1.6[b]
232 m^2/g^d

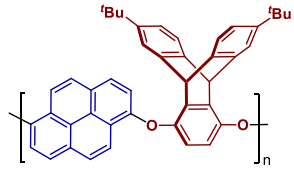

P8
X=Br 75% yield
Mn = 4.1 kg/mol, *Đ* = 1.5[b]
299 m^2/g^d

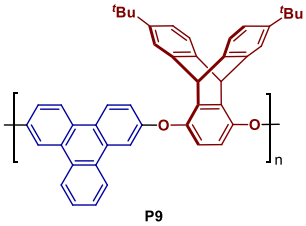

P9
X=Br 96% yield
Mn = 30.0 kg/mol, *Đ* = 2.3[b]
129 m^2/g^d

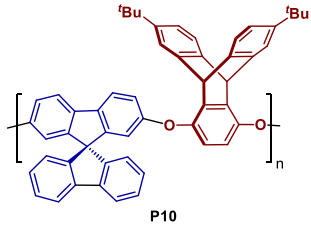

P10
X=Br 95% yield
Mn = 33.5 kg/mol, *Đ* = 1.6[b]
X=Cl 95% yield
Mn = 28.3 kg/mol, *Đ* = 1.7[c]
458 m^2/g^d

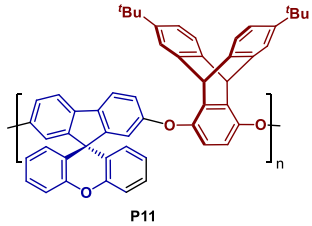

P11
X=Br 96% yield
Mn = 30.0kg/mol, *Đ* = 2.0[b]
225 m^2/g^d

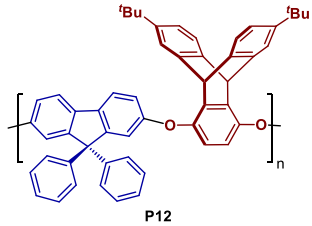

P12
X=Br 94% yield
Mn = 27.6 kg/mol, *Đ* = 1.9[b]
89 m^2/g^d

c) Synthesis of PAEs by using heteroaryl chlorides or bromides

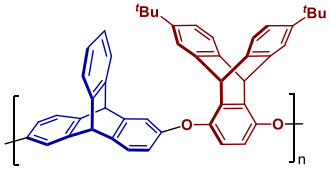

P13
X=Br 93% yield
Mn = 9.7 kg/mol, *Đ* = 1.4[b]
254 m^2/g^d

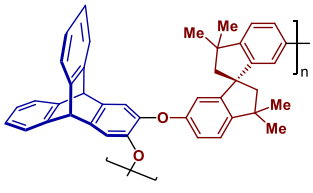

P14
X=Br 60% yield
Mn = 3.3 kg/mol, *Đ* = 1.3[b]
38 m^2/g^d

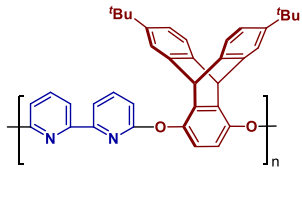

P15
X=Br 96% yield
Mn = 18.5 kg/mol, *Đ* = 1.8[b]
217 m^2/g^d

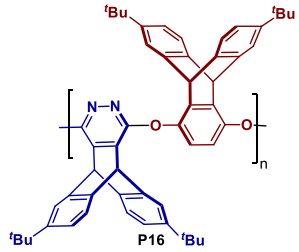

P16
X=Cl 94% yield
Mn = 17.8 kg/mol, *Đ* = 1.5[b]
492 m^2/g^d

[a]Aryl halide **A** (0.5 mmol), bisphenol **B** (0.5 mmol), $[(cinnamyl)PdCl]_2$ (0.5 mol %), ligand ^{t}BuXPhos (3.0 mol %), K_3PO_4 (3.0 equiv), 2-MeTHF (1.0 mL), 120 °C, 20−48 h. M_n and *Đ* were measured by THF GPC. [b]$[(Cinnamyl)PdCl]_2$ (1.0 mol %), ligand ^{t}BuBrettPhos (6.0 mol %), Tol/DME (0.6/0.3 mL), 140 °C, 20−72 h. M_n and *Đ* were measured by THF GPC. [c]$[(Cinnamyl)PdCl]_2$ (1.0 mol %), ligand ^{t}BuXPhos (6.0 mol %), Tol/DME (0.6/0.3 mL), 140 °C, 20 h. M_n and *Đ* were measured by THF GPC. [d]Brunauer−Emmett−Teller (BET) surface areas of the polymers were measured with N_2 sorption at 77 K.

based poly(arylene ether)s have been previously prepared by S_NAr polycondensations of triptycene containing phenols and activated aryl difluorides (such as decafluorobiphenyl, 4,4′-difluorobenzophenone, and bis(4-fluorophenyl) sulfone).[12,13] Our Pd-catalyzed C−O polycondensation now enables the preparation of triptycene-based PAEs using a wide range of aryl bromides or chlorides. To demonstration this fact, we synthesized a number of triptycene-based porous organic polymers using activated aryl dichlorides and dibromides (Table 2a). Triptycene-based poly(ether ether ketone) **P2** and poly(ether ether ketimine) **P3** were obtained as high molecular weight polymers using 4,4′-dichlorobenzophenone and its Schiff base derivative, respectively. Brunauer−Emmett−Teller (BET) analysis for **P2** and **P3** was unable to give meaningful

https://doi.org/10.1021/jacs.1c05853
J. Am. Chem. Soc. 2021, 143, 11828−11835

Table 3. Competition Experiments between Pd-Catalyzed C−O Polycondensation and S_NAr Reaction

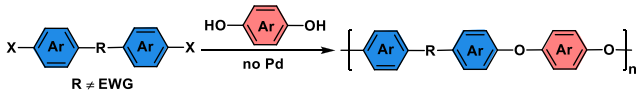

entry	P	X−Aryl−X	Pd C−O	condition A[a]	condition B[b]
1	**P9**	Br	M_n = 30.0 kg/mol, $Đ$ = 2.3	M_n = 0.9 kg/mol, $Đ$ = 1.5	M_n = 1.4 kg/mol, $Đ$ = 1.5
2	**P10**	Br	M_n = 33.5 kg/mol, $Đ$ = 1.6	M_n = 0.4 kg/mol, $Đ$ = 1.1	M_n = 0.9 kg/mol, $Đ$ = 1.3
3	**P10**	Cl	M_n = 28.3 kg/mol, $Đ$ = 1.7	M_n = 0.4 kg/mol, $Đ$ = 1.1	M_n = 1.0 kg/mol, $Đ$ = 1.1

[a]Condition A: **A** (0.5 mmol), **B** (0.5 mmol), K_3PO_4 (3.0 equiv), Tol/DME (0.6/0.3 mL), 140 °C, 72 h. [b]Condition B: **A** (0.5 mmol), **B** (0.5 mmol), K_3PO_4 (3.0 equiv), DMA (0.9 mL), 170 °C, 72 h. M_n and $Đ$ were measured by THF GPC. DMA = dimethylacetamide

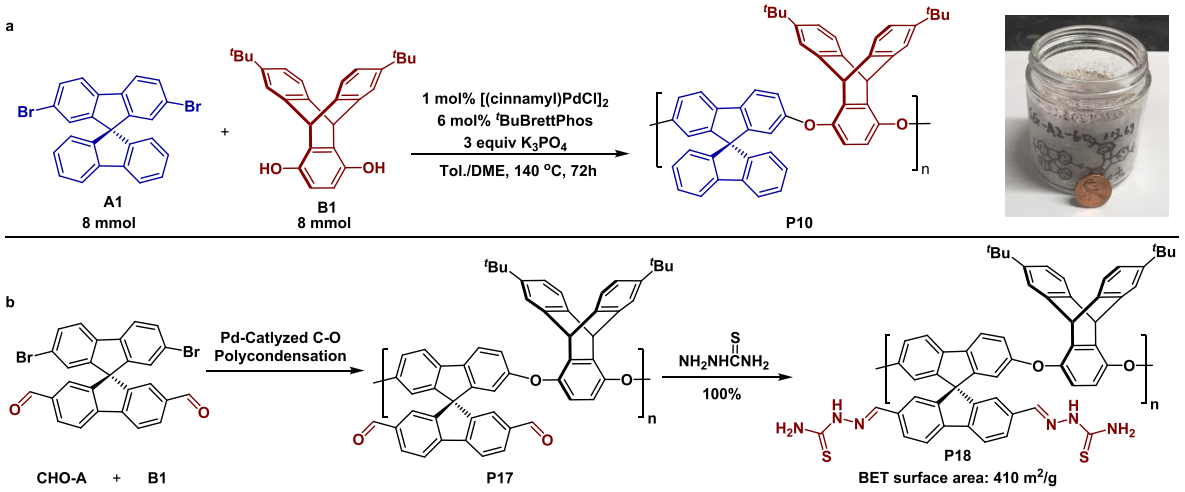

Figure 2. Extensions of Pd-catalyzed C−O polycondensation: (a) 8 mmol scale synthesis of poly(arylene ether)s, 5.6 g of **P10** was obtained from bulk polymerization (M_n = 47.7 kg/mol, $Đ$ = 1.7). (b) Preparation of functionalized porous poly(arylene ether) **P18**.

data since they have very low surface areas. The additional ^{t}Bu groups in **P4** afforded improved solubility relative to **P2** and yielded a higher molecular weight. BET analysis showed **P4**'s surface area to be 38 m^2/g (Table 2a). This low, but significant, surface area indicates that ^{t}Bu-triptycene groups are effective for increasing the BET surface area.

To create materials with even higher surface areas and/or functionality, we examined polycondensation reactions between $(^t\text{Bu})_2$-triptycene hydroquinone and other aryl dihalides that promote free volume, metal binding, and/or electronic properties. Commercially available aryl dibromides that contain electronically delocalized planar polycyclic aromatic structures, such as naphthalene (**P5**), phenanthrene (**P6**), pyrene (**P7**, **P8**), and triphenylene (**P9**), were used for the synthesis of new porous structures. We found that these unactivated aryl dibromides produce PAEs. The relatively low molecular weight of **P7** and **P8** was the result of limited solubility under the reaction conditions. BET analysis of these products indicated that the combination of $(^t\text{Bu})_2$-triptycene and planar polyaromatic structures increased the BET surface area to 200−300 m^2/g (**P6−8**, Table 2b).

In addition to the planar polycyclic aromatic structures, the nonplanar spirobifluorene (SBF) motif was also investigated. SBF is a common 3D substructure known to inhibit the efficient packing between polymer chains and increase the free volume.[23] The commercially available 2,7-dibromo-9,9′-spirobifluorene as well as the easily prepared 2,7-dichloro-9,9′-spirobifluorene both produced **P10** of similar molecular weight. **P10** has high molecular weight and a molecular weight distribution expected for a well-behaved step-growth polymerization. Notably, the BET surface area of **P10** was 458 m^2/g, which is much higher than that of triptycene-containing polymers lacking spirobifluorene units. Two more analogues of 2,7-dibromo-9,9′-spirobifluorene were used to produce **P11** and **P12**. However, both polymers display lower BET surface areas than **P10**. Furthermore, to expand the scope of highly rigid aryl halides, 2,6-dibromotriptycene and 2,3-dibromotriptycene were used to produce **P13** and **P14**. Although **P14** has a lower molecular weight and BET surface area, its preparation indicated that the Pd-catalyzed C−O coupling protocol can accommodate 1,2-substituted aryl dibromides. We also produced PAEs with nitrogen-containing heterocycles with $(^t\text{Bu})_2$-triptycene comonomers (Table 2c). We found that the reaction conditions are compatible with bipyridine and pyridazine, producing **P15** and **P16** in good yields. The bipyridine polymer, **P15**, is soluble in chloroform and THF at room temperature and has a BET surface area of 217 m^2/g. The pyridazine-containing polymer **P16** has an all-iptycene backbone, resulting in a highly rigid structure with a high BET surface area of 492 m^2/g. Furthermore, we also evaluated the thermostability of the polymers (**P1−16**) by thermogravimetric analysis. Their TGA thermographs, shown in Figure S6 (Supporting Information), indicated that **P4−16** exhibited excellent thermostability (T_d > 400 °C)

Competition experiments between Pd-catalyzed C−O polycondensation and S_NAr reaction were carried out to display the efficiency of our new method. We found that the polycondensation reaction for the synthesis of **P9** and **P10** without the presence of Pd catalyst only afforded low molecular weight oligomeric products (Table 3). Although it

https://doi.org/10.1021/jacs.1c05853
J. Am. Chem. Soc. 2021, 143, 11828−11835

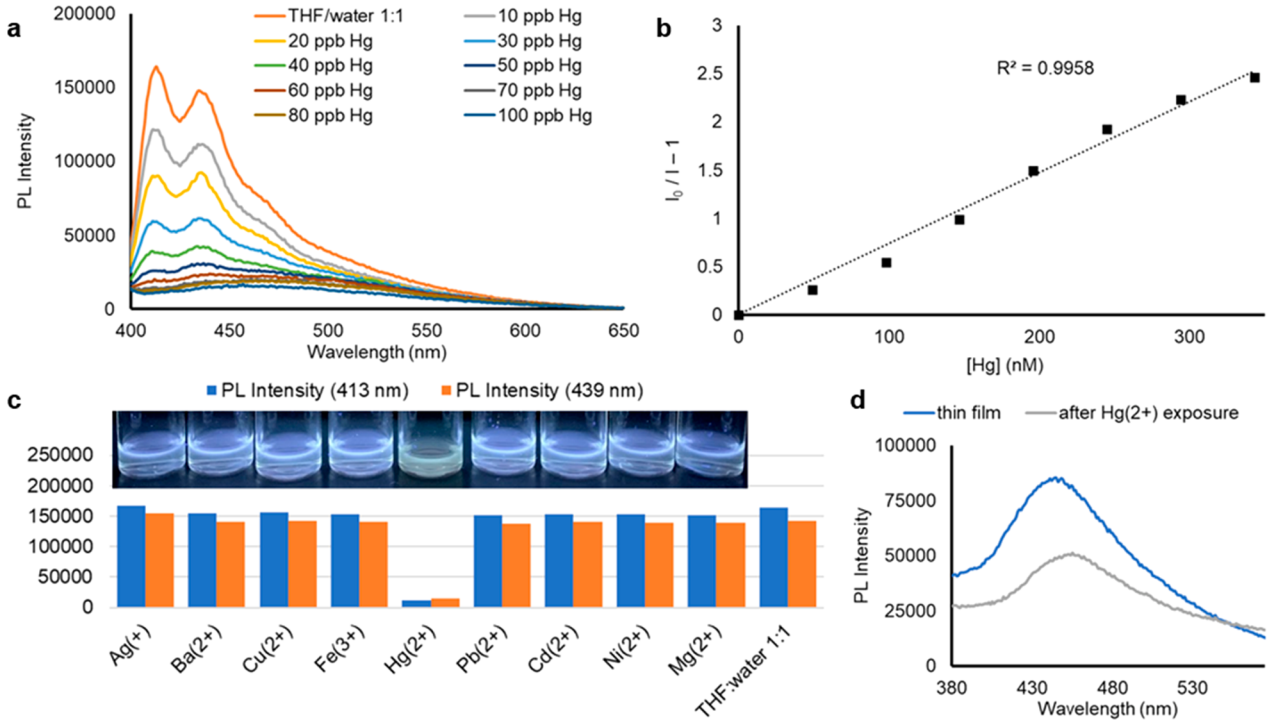

Figure 3. Application of porous poly(arylene ether) as a fluorescent Hg^{2+} sensor. (a) Fluorescence titration of $HgCl_2$ into a solution of **P18** in 1:1 THF/water (λ_{exc} = 350 nm). (b) Stern–Volmer plot for determination of the Hg^{2+} binding constant. (c) Specificity of the fluorescent sensor for Hg^{2+} over other common cations. Hand-held long-wave UV lamp (λ_{exc} = 365 nm) was used to produce the photograph. (d) Use of **P18** as a thin film sensor.

is known that a significant S_NAr reaction can take place at 170 °C in highly polar solvent (DMA),[28] the M_n of the product was still low under these conditions (Table 3, entries 1 and 2). Aryl chlorides are generally more active substrates than aryl bromides in S_NAr reactions.[29] However, the polycondensation reaction of aryl chlorides without the presence of Pd catalysis did not proceed significantly at either 140 or 170 °C (Table 3, entry 3).

To demonstrate the scalability of the PAE synthesis, we performed the synthesis of poly(arylene ether) **P10** on a 5 g scale. A polymerization with 8 mmol of commercially available 2,7-dibromo-9,9′-spirobifluorene and 8 mmol of $(^tBu)_2$-triptycene hydroquinone was carried out at 140 °C in a pressure vessel. Poly(arylene ether) **P10** was obtained as a gray fibrous material in very high yield (5.6 g, 98% yield, Figure 2a). GPC analysis revealed a M_n of 47.7 kg/mol ($Đ$ = 1.7), which was higher than that of the **P10** product obtained at a 1.0 mmol scale (M_n = 33.5 kg/mol, $Đ$ = 1.6, Table 2b). ICP-MS of the polymer product showed that the Pd residue in the polymer is 16 ppm by weight, indicating that the majority of Pd had been removed during the purification process.

POPs with designed functional groups have emerged as a versatile platform for many potential applications, such as catalysis, sensing, and purification.[1,3,30,31] Our new bottom-up approach allows the installation of functionality using an elaborated monomer. Hence, we prepared aldehyde-containing PAE **P17** (93% yield, M_n = 11.8 kg/mol, $Đ$ = 3.2) using the functionalized aryl dibromide monomer (Figure 2b). Demonstrating the synthetic flexibility of the aldehyde groups, the aldehyde-containing polymer **P17** can be converted to various porous polymers with functional properties. For instance, the thiosemicarbazide (TSC) group, known to efficiently bind Hg^{2+},[32,33] was condensed quantitatively onto the porous PAE structure via postmodification to give **P18** with a 410 m^2/g BET surface area (Figure 2b). We envisioned that this TSC-containing porous poly(arylene ether) **P18** may be used as a fluorescence sensor for detecting and quantifying dissolved Hg^{2+}. **P18** was soluble in many organic solvents as well as an equal mixture of THF and water. Upon excitation at 350 nm, the polymer exhibited bright fluorescence at λ_{max} = 413 nm with a fluorescence quantum yield of 2.5%. Upon titration with Hg^{2+} ions, the fluorescence was rapidly quenched (Figure 3a), as has been observed previously with chromophores bearing a thiosemicarbazone moiety.[33,34] The binding constant K_a was determined to be 7.4 × 10^6, and the theoretical limit of detection based on the fluorescence quenching is calculated to be 0.58 ppb (Figure 3b). This sensing behavior is specific for Hg^{2+} over several other cations (Figure 3c), as demonstrated by exposure of the polymer to 1.0 ppm solutions of various metal salts in a THF–water mixture. Drop-cast smooth films of **P18** were produced by slow evaporation and displayed fluorescence at a slightly red-shifted wavelength (λ_{max} = 431 nm) relative to that in a THF/water solution (Figure 3d). Upon soaking of this film in a 0.50 ppm aqueous solution of $HgCl_2$ for 30 min, the fluorescence was found to be attenuated and also noticeably red shifted. These experiments suggest the potential of postfunctionalized porous poly(arylene ether) compounds to serve as easily accessible and efficient fluorescence sensors.

Mercury-ion contamination in water is global health issue as a result of industrial emissions.[35] Porous materials with a high Hg^{2+} adsorption capacity and reusability are highly desired. Thus, we considered whether the TSC-containing porous PAE **P18** could also be used as an Hg^{2+} adsorbent for water purification. To assess the overall efficiency of Hg^{2+} uptake by **P18**, 5 mg of this polymer was exposed for 24 h to aqueous

https://doi.org/10.1021/jacs.1c05853
J. Am. Chem. Soc. 2021, 143, 11828–11835

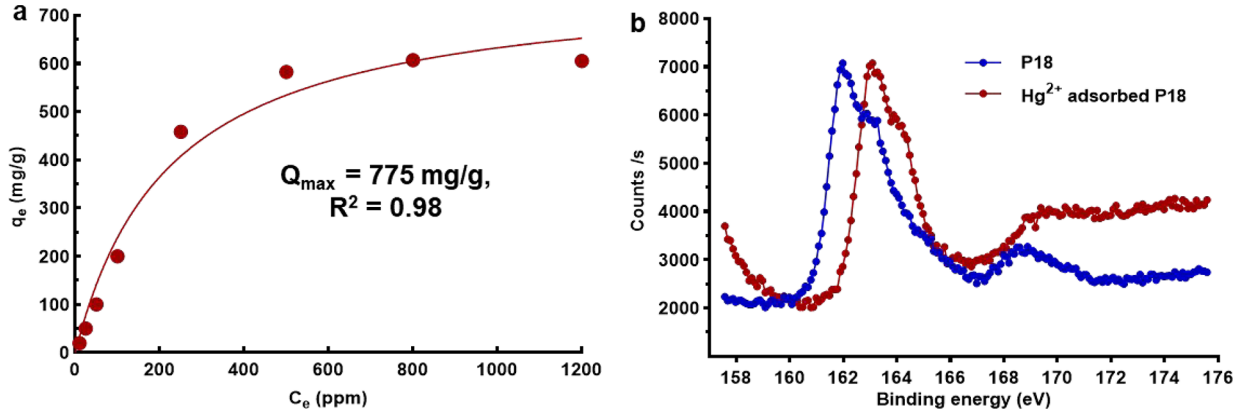

Figure 4. Application of porous poly(arylene ether) for Hg^{2+} removal. (a) Hg^{2+} adsorption isotherms. Langmuir nonlinear isotherm model fitting leads to the determination of a maximum adsorption capacity (Q_{max}) of 775 mg g^{-1} when high concentrations (in the range 25−1200 ppm) of Hg^{2+} were used. (b) S 2p XPS spectra of pristine (blue) and Hg^{2+}-adsorbed **P18** (red).

$HgCl_2$ solutions with initial concentrations in the range of 25−1200 ppm. **P18** exhibits a very high adsorption for Hg^{2+}, which was quantified by fitting the equilibrium adsorption data to the nonlinear Langmuir model (Figure 4a).[36] Remarkably, the polymer was estimated to have a capacity of 775 mg of Hg^{2+} per gram of polymer, which compares favorably to the current reported porous materials for mercury removal (Table S1).[37−44] In addition, **P18** can be easily regenerated by soaking in thiourea solution at room temperature (Figure S7-1). Moreover, to confirm the chemical interaction between the polymer and the Hg^{2+} ions, we analyzed **P18** by X-ray photoelectron spectroscopy (XPS) before and after Hg^{2+} exposure. The analysis of the sulfur (S 2p) atoms shows a notable peak at 162.0 eV for pristine **P18**. Upon Hg^{2+} exposure, this resonance was shifted to 163.0 eV, which is attributed to sulfur−Hg^{2+} complex formation (Figure 4b).[45] The application of **P18** as a Hg^{2+} fluorescent sensor and material for Hg^{2+} removal highlights the versatility of the functional POPs accessible through our polycondensation process. We believe that the synthetic strategy will enable the rational design of new functional porous poly(arylene ether)s for many other applications.

CONCLUSION

In summary, we developed a methodology to synthesize porous poly(arylene ether)s which are not accessible by traditional S_NAr methods. The Pd-catalyzed C−O polycondensation reaction allows the synthesis of PAEs using available aryl chlorides and bromides lacking anion-stabilizing groups at the ortho and/or para positions. The synthetic flexibility of this reaction enables us to combine bisphenols and aryl dihalides that promote free volume in PAEs. Functional porous PAEs can be rationally designed and prepared via this new synthetic methodology. TSC-containing porous PAEs were designed for the detection of Hg^{2+} and its removal from water. This access to porous PAEs with designed functional groups provides a new bottom-up approach for generating versatile solution-processable functional materials. Our ongoing work will focus on developing porous PAEs for other applications.

ASSOCIATED CONTENT

Supporting Information

The Supporting Information is available free of charge at https://pubs.acs.org/doi/10.1021/jacs.1c05853.

Instrumentation and materials, detailed experimental procedures, details of the characterization of the polymers and monomers, ^1H and ^{13}C NMR spectra, GPC chromatograms, N_2 adsorption−desorption isotherm, X-ray photoelectron spectroscopy (PDF)

AUTHOR INFORMATION

Corresponding Author

Timothy M. Swager − *Department of Chemistry, Massachusetts Institute of Technology, Cambridge, Massachusetts 02139, United States;* orcid.org/0000-0002-3577-0510; Email: tswager@mit.edu

Author

Sheng Guo − *Department of Chemistry, Massachusetts Institute of Technology, Cambridge, Massachusetts 02139, United States;* orcid.org/0000-0002-2542-0525

Complete contact information is available at: https://pubs.acs.org/10.1021/jacs.1c05853

Notes

The authors declare the following competing financial interest(s): We will be filing a patent.

ACKNOWLEDGMENTS

This research was supported by the National Science Foundation DMR-1809740 and KAUST sensor project REP-2719. The authors thank Dr. Richard Y. Liu for advice on the preparation of this paper and fluorescence titration experiment, Lennon Shaoxiong Luo for XPS analysis, and a core center grant P30-ES002109 from the National Institute of Environmental Health Sciences, National Institutes of Health for ICP-MS equipment.

REFERENCES

(1) Kitagawa, S. Future Porous Materials. *Acc. Chem. Res.* **2017**, *50*, 514−516.

(2) Wu, D.; Xu, F.; Sun, B.; Fu, R.; He, H.; Matyjaszewski, K. Design and Preparation of Porous Polymers. *Chem. Rev.* **2012**, *112*, 3959−4015.

(3) Slater, A. G.; Cooper, A. I. Porous Materials. Function-Led Design of New Porous Materials. *Science* **2015**, *348*, aaa8075.

(4) Das, S.; Heasman, P.; Ben, T.; Qiu, S. Porous Organic Materials: Strategic Design and Structure-Function Correlation. *Chem. Rev.* **2017**, *117*, 1515−1563.

(5) Ghanem, B. S.; Swaidan, R.; Litwiller, E.; Pinnau, I. Ultra-Microporous Triptycene-based Polyimide Membranes for High-Performance Gas Separation. *Adv. Mater.* **2014**, *26*, 3688−3692.
(6) Zhou, H.; Jin, W. Membranes with Intrinsic Micro-Porosity: Structure, Solubility, and Applications. *Membranes* **2019**, *9*, 3.
(7) McKeown, N. B. Polymers of Intrinsic Microporosity (PIMs). *Polymer* **2020**, *202*, 122736.
(8) Budd, P. M.; Ghanem, B. S.; Makhseed, S.; McKeown, N. B.; Msayib, K. J.; Tattershall, C. E. Polymers of Intrinsic Microporosity (PIMs): Robust, Solution-Processable, Organic Nanoporous Materials. *Chem. Commun.* **2004**, 230−231.
(9) In *Molecular Basis of Transitions and Relaxations*; Meier, D. J., Ed.; Midland Macromolecular Monographs; Gordon and Breach, 1978; Vol. *4*, p 429.
(10) Yee, A. F.; Smith, S. A. Molecular Structure Effects on the Dynamic Mechanical Spectra of Polycarbonates. *Macromolecules* **1981**, *14*, 54−64.
(11) Swager, T. M. Iptycenes in the Design of High-Performance Polymers. *Acc. Chem. Res.* **2008**, *41*, 1181−1189.
(12) Moh, L. C. H.; Goods, J. B.; Kim, Y.; Swager, T. M. Free Volume Enhanced Proton Exchange Membranes from Sulfonated Triptycene Poly(ether ketone). *J. Membr. Sci.* **2018**, *549*, 236−243.
(13) Long, T. M.; Swager, T. M. Molecular Design of Free Volume as a Route to Low-κ Dielectric Materials. *J. Am. Chem. Soc.* **2003**, *125*, 14113−14119.
(14) Thomas, S. W., III; Long, T. M.; Pate, B. D.; Kline, S. R.; Thomas, E. L.; Swager, T. M. Perpendicular Organization of Macromolecules: Synthesis and Alignment Studies of a Soluble Poly(iptycene). *J. Am. Chem. Soc.* **2005**, *127*, 17976−17977.
(15) Long, T. M.; Swager, T. M. Using "Internal Free Volume" to Increase Chromophore Alignment. *J. Am. Chem. Soc.* **2002**, *124*, 3826−3827.
(16) Salvi, L.; Davis, N. R.; Ali, S. Z.; Buchwald, S. L. A New Biarylphosphine Ligand for the Pd-Catalyzed Synthesis of Diaryl Ethers under Mild Conditions. *Org. Lett.* **2012**, *14*, 170−173.
(17) Aranyos, A.; Old, D. W.; Kiyomori, A.; Wolfe, J. P.; Sadighi, J. P.; Buchwald, S. L. Novel Electron-Rich Bulky Phosphine Ligands Facilitate the Palladium-Catalyzed Preparation of Diaryl Ethers. *J. Am. Chem. Soc.* **1999**, *121*, 4369−4378.
(18) Burgos, C. H.; Barder, T. E.; Huang, X.; Buchwald, S. L. Significantly Improved Method for the Pd-Catalyzed Coupling of Phenols with Aryl Halides: Understanding Ligand Effects. *Angew. Chem., Int. Ed.* **2006**, *45*, 4321−4326.
(19) Koizumi, T.-a.; Kanbara, T. Cross-Coupling Polymerization. In *Organometallic Reactions and Polymerization*; Osakada, K., Ed.; Springer Berlin Heidelberg: Berlin, Heidelberg, 2014; pp 271−301.
(20) Rose, I.; Bezzu, C. G.; Carta, M.; Comesana-Gandara, B.; Lasseuguette, E.; Ferrari, M. C.; Bernardo, P.; Clarizia, G.; Fuoco, A.; Jansen, J. C.; Hart, K. E.; Liyana-Arachchi, T. P.; Colina, C. M.; McKeown, N. B. Polymer Ultrapermeability from the Inefficient Packing of 2D Chains. *Nat. Mater.* **2017**, *16*, 932−937.
(21) Shamsabadi, A. A.; Seidi, F.; Nozari, M.; Soroush, M. A New Pentiptycene-Based Dianhydride and Its High-Free-Volume Polymer for Carbon Dioxide Removal. *ChemSusChem* **2018**, *11*, 472−482.
(22) Bezzu, C. G.; Carta, M.; Tonkins, A.; Jansen, J. C.; Bernardo, P.; Bazzarelli, F.; McKeown, N. B. A Spirobifluorene-Based Polymer of Intrinsic Microporosity with Improved Performance for Gas Separation. *Adv. Mater.* **2012**, *24*, 5930−5933.
(23) Chen, Q.; Wang, J.-X.; Wang, Q.; Bian, N.; Li, Z.-H.; Yan, C.-G.; Han, B.-H. Spiro(fluorene-9,9'-xanthene)-Based Porous Organic Polymers: Preparation, Porosity, and Exceptional Hydrogen Uptake at Low Pressure. *Macromolecules* **2011**, *44*, 7987−7993.
(24) Carta, M.; Malpass-Evans, R.; Croad, M.; Rogan, Y.; Jansen, J. C.; Bernardo, P.; Bazzarelli, F.; McKeown, N. B. An Efficient Polymer Molecular Sieve for Membrane Gas Separations. *Science* **2013**, *339*, 303−307.
(25) Shukla, D.; Negi, Y. S.; Uppadhyaya, J. S.; Kumar, V. Synthesis and Modification of Poly(ether ether ketone) and their Properties: A Review. *Polym. Rev.* **2012**, *52*, 189−228.
(26) Roovers, J.; Cooney, J. D.; Toporowski, P. M. Synthesis and Characterization of Narrow Molecular-Weight Distribution Fractions of Poly(aryl ether ether ketone). *Macromolecules* **1990**, *23*, 1611−1618.
(27) Percec, V.; Clough, R. S.; Rinaldi, P. L.; Litman, V. E. Termination by Reductive Elimination in the Polyetherification of Bis(aryl chlorides) Activated by Carbonyl Groups, with Bisphenolates. *Macromolecules* **1991**, *24*, 5889−5892.
(28) Gazitúa, M.; Tapia, R. A.; Contreras, R.; Campodónico, P. R. Effect of the Nature of the Nucleophile and Solvent on an SNAr Reaction. *New J. Chem.* **2018**, *42*, 260−264.
(29) Terrier, F. *Modern Nucleophilic Aromatic Substitution*; Wiley-VCH, 2013.
(30) Zhang, W.; Aguila, B.; Ma, S. Potential Applications of Functional Porous Organic Polymer Materials. *J. Mater. Chem. A* **2017**, *5*, 8795−8824.
(31) Rivero-Crespo, M.; Toupalas, G.; Morandi, B. Preparation of Versatile, Porous Poly-Arylthioethers by Reversible Pd-Catalysed C−S/C−S Metathesis. *ChemRxiv*, **2021** DOI: 10.26434/chemrxiv.14075390.v1 (accessed 2021−02−25).
(32) Ahmed, S. A. Alumina Physically Loaded by Thiosemicarbazide for Selective Preconcentration of Mercury(II) Ion from Natural Water Samples. *J. Hazard. Mater.* **2008**, *156*, 521−529.
(33) Haldar, U.; Lee, H.-i. BODIPY-Derived Polymeric Chemosensor Appended with Thiosemicarbazone Units for the Simultaneous Detection and Separation of Hg(II) Ions in Pure Aqueous Media. *ACS Appl. Mater. Interfaces* **2019**, *11*, 13685−13693.
(34) Li, Y.; He, Y.; Guo, F.; Zhang, S.; Liu, Y.; Lustig, W. P.; Bi, S.; Williams, L. J.; Hu, J.; Li, J. NanoPOP: Solution-Processable Fluorescent Porous Organic Polymer for Highly Sensitive, Selective, and Fast Naked Eye Detection of Mercury. *ACS Appl. Mater. Interfaces* **2019**, *11*, 27394−27401.
(35) Wang, J.; Feng, X.; Anderson, C. W. N.; Xing, Y.; Shang, L. Remediation of Mercury Contaminated Sites − A Review. *J. Hazard. Mater.* **2012**, *221*−*222*, 1−18.
(36) García-Zubiri, I. X.; González-Gaitano, G.; Isasi, J. R. Sorption Models in Cyclodextrin Polymers: Langmuir, Freundlich, and a Dual-Mode Approach. *J. Colloid Interface Sci.* **2009**, *337*, 11−18.
(37) Shetty, D.; Boutros, S.; Eskhan, A.; De Lena, A. M.; Skorjanc, T.; Asfari, Z.; Traboulsi, H.; Mazher, J.; Raya, J.; Banat, F.; Trabolsi, A. Thioether-Crown-Rich Calix[4]arene Porous Polymer for Highly Efficient Removal of Mercury from Water. *ACS Appl. Mater. Interfaces* **2019**, *11*, 12898−12903.
(38) Huang, N.; Zhai, L.; Xu, H.; Jiang, D. Stable Covalent Organic Frameworks for Exceptional Mercury Removal from Aqueous Solutions. *J. Am. Chem. Soc.* **2017**, *139*, 2428−2434.
(39) Sun, Q.; Aguila, B.; Perman, J.; Earl, L. D.; Abney, C. W.; Cheng, Y.; Wei, H.; Nguyen, N.; Wojtas, L.; Ma, S. Postsynthetically Modified Covalent Organic Frameworks for Efficient and Effective Mercury Removal. *J. Am. Chem. Soc.* **2017**, *139*, 2786−2793.
(40) Li, B.; Zhang, Y.; Ma, D.; Shi, Z.; Ma, S. Mercury Nano-trap for Effective and Efficient Removal of Mercury(II) from Aqueous Solution. *Nat. Commun.* **2014**, *5*, 5537.
(41) Yee, K.-K.; Reimer, N.; Liu, J.; Cheng, S.-Y.; Yiu, S.-M.; Weber, J.; Stock, N.; Xu, Z. Effective Mercury Sorption by Thiol-Laced Metal−Organic Frameworks: in Strong Acid and the Vapor Phase. *J. Am. Chem. Soc.* **2013**, *135*, 7795−7798.
(42) Shin, Y.; Fryxell, G. E.; Um, W.; Parker, K.; Mattigod, S. V.; Skaggs, R. Sulfur-Functionalized Mesoporous Carbon. *Adv. Funct. Mater.* **2007**, *17*, 2897−2901.
(43) Xu, D.; Wu, W. D.; Qi, H.-J.; Yang, R.-X.; Deng, W.-Q. Sulfur Rich Microporous Polymer Enables Rapid and Efficient Removal of Mercury(II) from Water. *Chemosphere* **2018**, *196*, 174−181.
(44) Mon, M.; Lloret, F.; Ferrando-Soria, J.; Martí-Gastaldo, C.; Armentano, D.; Pardo, E. Selective and Efficient Removal of Mercury from Aqueous Media with the Highly Flexible Arms of a BioMOF. *Angew. Chem., Int. Ed.* **2016**, *55*, 11167−11172.

(45) Walton, R. A. The X-Ray Photoelectron Spectra of Metal Complexes of Sulfur-Containing Ligands: Sulfur 2p Binding Energies. *Coord. Chem. Rev.* **1980**, *31*, 183−220.

https://doi.org/10.1021/jacs.1c05853
J. Am. Chem. Soc. 2021, 143, 11828−11835